Dusty cloud properties and radiative forcing over dust source and remote regions derived from CERES/CALIPSO during PACDEX

Wencai Wang[1], Jianping Huang[1], Patrick Minnis[2], Yongxiang Hu[2]

Jiming Li[1], Zhongwei Huang[1] and J. Kirk Ayers[3]

[1] Key Laboratory for Semi-Arid Climate Change of the Ministry of Education,

College of Atmospheric Sciences, Lanzhou University, Lanzhou, 730000

[2]NASA Langley Research Center, Hampton, VA, 23666

[3]SSAI, Hampton, One Enterprise Parkway, Hampton, VA, 23666

Submitted to: JGR CALIPSO Special Issue

Abstract

Dusty cloud properties and radiative forcing (RF) over northwestern China (source region) are compared to those over the northeastern Pacific (remote region) during PACDEX (March 2007 to May 2007) using CALIPSO (Cloud-Aerosol Lidar and Infrared Pathfinder Satellite Observations) level 2, MODIS CERES SSF version 2, and CloudSat level 2 data. Dusty clouds are defined as clouds extant in a dust plume environment (i.e., dust aerosols observed within 50 km of the cloud), while pure clouds are those in dust-free conditions. CALIPSO lidar and CloudSat radar measurements are used to discriminate between dusty and pure clouds in both study regions. It was found that dust aerosols change the microphysical characteristics of clouds, reducing cloud optical depth, liquid/ice water path (LWP/IWP), and effective droplet size. The decreased cloud optical depths and water paths diminish the cloud cooling effect, leading to a greater warming effect. The dust aerosols cause an instantaneous net cloud cooling effect reduction of 43.4% and 16.7% in the source and remote regions, respectively. The dust aerosol effects appear to be greater for ice clouds than for liquid water clouds in the remote region. These results are consistent with PACDEX aircraft observations.

1. Introduction

Asian dust storms can have significant impacts on the global climate system. These storms originate in the Taklimakan Desert of China and the Gobi Desert of Mongolia, most frequently in late winter and early spring. During an average year, sandstorms are observed on more than 20 days, while blowing sand occurs twice as often [*Zhou et al.,* 2001]. *Li et al.* [2004] estimate that the annual mean dust emission from China is about 800 kilotons. Besides contributing to regional and global climate change, dust aerosols affect the biosphere since they deposit minerals and soil in the ocean and on remote land areas. They directly impact climate by scattering solar radiation and absorbing land-atmosphere long wave (LW) radiation. Dust outbreaks also alter cloud droplet concentrations by increasing cloud condensation nuclei abundance and subsequently affecting the microphysical properties and cloud life cycle [*Huang et al*., 2006a, b; *Niu et al*., 2001]. Using a two-dimensional spectral resolving cloud model, *Yin and Chen* [2007] simulated the effects of mineral dust particles on the development of cloud microphysics and precipitation over northern China. They showed that when dust particles are involved in cloud development as CCN (cloud condensation nuclei) and IN (ice nuclei) at the same time, the increased dust aerosol loading will suppress precipitation because the enhancement of CCN is nearly overwhelmed by the stronger suppressing effect of IN [*Chen et al*., 2007]. Furthermore, *Han et al*. [2008] found that the role of precipitation in suppressing dust storm occurrence is unimportant and that dust aerosols may play a more important role in suppressing the precipitation over arid and desert regions. This, in turn, could reduce the probability of precipitation, resulting in more complex and uncertain indirect effects.

Clouds are another important factor in climate change; about 60% of the Earth's surface is covered with clouds. On a global average basis, clouds cool the Earth-atmosphere system at the top-of-atmosphere (TOA). Measurements from the Earth Radiation Budget Experiment (ERBE) [*Collins et al*., 1994] indicate that small changes to cloud macro-physical (coverage, structure, altitude) and microphysical properties (droplet size, phase) have significant effects on climate. For instance, a 5% increase in shortwave (SW) cloud forcing would compensate for the increase in greenhouse gases that occurred during the period from 1750 through 2000 [*Ramaswamy et al*., 2001].

Due to frequent sandstorms, sand and dust are always present in the atmosphere over dust source regions and form the dust plumes in upper-layer atmosphere. These dust plumes often become entrained in westerlies and flow out from the continent to the open sea near Korea and Japan, and can impact the atmospheric hydrological and radiative budgets along the way [*Husar et al*., 2001; *Zhang et al*., 2003, *Huang et al*., 2008]. The effect of this mixed dust-pollution plume on the Pacific cloud systems and the associated radiative forcing is an outstanding problem for understanding climate change and has not been explored [*Stith et al*., 2009]. The primary reason that this problem has not been studied is the lack of sufficient measurements of the plume's evolution as it crosses the Pacific Ocean. The international PACific Dust EXperiment (PACDEX) attempted to fill this observational gap by taking airborne measurements of dust and pollution transported from the western to the eastern Pacific and into North America. Under the framework of this campaign, intensive observations were carried out during March through May 2007 [*Stith et al*., 2009]. Vertical profiles of clouds and aerosols were also measured remotely by the Cloud-Aerosol Lidar and Infrared Pathfinder Satellite Observations (CALIPSO) lidar [*Winker et al*., 2007] and the CloudSat [*Stephens et al*., 2002]. Those narrow cross-sections of the atmosphere were complemented TOA measurements of broadband fluxes

and retrievals of bulk cloud properties from the Clouds and the Earth's Radiant Energy System (CERES; see *Wielicki et al*. [1998]) that provide complete horizontal spatial coverage.

In this paper we present a study of the dust effect on cloud and RF over two different regions, the dust source region (northwestern China) and the PACDEX region (northeastern Pacific and Sea of Japan, hereafter remote region), during PACDEX (March 2007 to May 2007) using CALIPSO, CERES, and CloudSat measurements. Part of this study extends our previous research [*Huang et al.*, 2006a, b] that examined dusty and dust-free clouds (hereafter pure cloud) selected based on observations from surface meteorological stations in China and Mongolia. If no dust was observed at the surface the overlying cloud observed by the satellite was defined as pure cloud, but if the surface observation reported any dust event, the cloud was defined as a dusty cloud. This cloud selection procedure is not necessarily accurate because the dust and clouds could have occurred at different altitudes. CALIPSO/CloudSat, however, can observe aerosols and clouds at the same altitude [*Winker et al*., 2007; *Hu et al*., 2006, *Liu et al*., 2006, 2008; *Vaughan et al*., 2004; *Huang et al*., 2007] adding certainty that the dust can directly affect the clouds. In this study, the CALIPSO Lidar and CloudSat Radar measurements are used to identify dusty and pure clouds in both dust source and remote regions. Dusty clouds are defined as clouds that exist in a dust plume environment (i.e., dust aerosols observed within 50 km of the cloud), while pure clouds are clouds in a dust-free environment. The CALIPSO/CloudSat measurements, used in conjunction with the CERES data, should lead to reliable analysis of dust aerosol effect on cloud and RF over the PACDEX area, and expand our understanding of their impact on climate.

2. Data and Method

This study uses CALIPSO lidar level 2, Aqua CERES, and CloudSat observations taken between March and May 2007. All three satellites, part of the A-Train formation, are in Sun-synchronous orbits with equatorial crossing times close to 0130/1430 LST. Since the orbital separation of these satellites is very small they have closely matched temporal sampling and facilitate the merging of their respective datasets. CALIPSO acquires near-nadir vertical profiles of elastic backscatter at two wavelengths (532 and 1064 nm) during both day and night phases of the orbit. CALIPSO also provides profiles of linear depolarization at 532 nm used to discriminate between ice and water clouds, and to identify non-spherical aerosol particles. The primary products are three calibrated and geolocated lidar profiles – 532 nm and 1064 nm pure attenuated backscatter and 532 nm perpendicular polarization component. Depolarization ratio is computed directly from the ratio of two polarization components of the attenuated backscatter at 532 nm. The CALIPSO lidar level 2 data product (version 1.xx) contains the cloud and aerosol layer reports along with column properties. Level 1B data is first averaged to 5 km. The 5 km cloud layer products are used to screen out cloudy profiles [*Liu et al.*, 2008].

The CERES Single Scanner Footprints (SSF) data used here combine CERES radiation measurements, imager-based cloud microphysical retrievals, and ancillary meteorology and aerosol fields to form a comprehensive, high-quality compilation of satellite-derived cloud, aerosol, and radiation budget information for radiation and climate studies. Of the roughly 160 parameters in the SSF data set, the current analysis uses the following: TOA shortwave and longwave fluxes, and cloud ice water path (IWP), liquid water path (LWP), top effective temperature, effective droplet radius (Re) or ice crystal diameter (De), and optical depth (OPD). The CERES instrument measures broadband radiances at the TOA in three spectral regions, shortwave (SW, 0.2 - 5.0 μm), window (8 - 14 μm), and longwave (LW, 5 - 100 μm) with a spatial resolution of about 20 km at nadir. These radiances are

converted to TOA fluxes with a scene identification algorithm and angular distribution models [*Loeb et al*., 2005]. Flux measurements from CERES are used to estimate the instantaneous cloud RF. The CERES cloud properties were retrieved from 1-km resolution MODerate Resolution Imaging Spectroradiometer (MODIS) using the methods of *Minnis et al*. [2008, 2009].

Humidity fields are taken from the reanalysis product of the National Centers for Environmental Prediction (NCEP). The NCEP/NCAR (National Center for Atmospheric Research) reanalysis project uses a state-of-the-art global numerical weather analysis/forecast system to perform data assimilation using historical observations, spanning the time period from 1957 to the present [*Kalnay et al*., 1996]. The model used in the NCEP reanalysis has 28 vertical levels extending from the surface to 40 km, with vertical resolution of 2 km near the tropical tropopause [*William et al*., 2000].

3. Dusty cloud identification

Dusty clouds are defined as clouds that exist in a dust plume environment (i.e., dust aerosols observed within 50 km of the cloud). The CALIPSO Level-2 data are used as the primary cloud identification tool with confirmation from CloudSat cloud mask data, which are from the 2B-GEOPROF product restricted to cloud confidence ≥20 [*Mace et al*., 2007]. The CALIPSO level-2 analysis identifies layers of enhanced backscatter as either aerosols or clouds. Here, we define the clouds as dusty clouds if the aerosol and cloud layers are at the same height or the height difference (such as the height difference between the base height for cloud layer and the top height for aerosol layer) between them is within 50 m in the same areas, and the aerosols are dust aerosols. The CALIPSO lidar Level 2 Vertical Feature Mask (VFM) product, which describes the vertical and horizontal distribution of cloud and aerosol layers, is used to distinguish dust from other types of

aerosols. In addition, the identification of dust aerosols in a given altitude range of a lidar profile is accomplished by checking the volume depolarization ratio (VDR). The depolarization ratio of dust is high due to the non-spherical shape of the dust particles. For other types of aerosols the depolarization ratio is low (close to zero). Therefore, the depolarization ratio is used as an indicator to separate dust from other aerosol types [*Murayama et al*., 2001]. A threshold of 0.06 is used to detect the dust layer *Liu et al*. [2008] provide a detailed description of the CALIPSO data processing.

To examine cloud modification induced by dust aerosols, the dust source and remote regions were selected to investigate clouds in different regions. The dust source region extends from 35° N to 45° N and 70° E to 110° E, and the remote region is bound by 35 and 45° N and 120 and 160° E (Figure 1). Figure 2 shows a typical dusty cloud observation, taken March 5, 2007, in the source region. The red areas in Figure 2a are identified as clouds, but with very low confidence, by CloudSat. Figures 2b, 2c, and 2d, respectively, show plots of CALIPSO attenuated backscatter at 532 nm, VDR and the backscatter color ratio (defined as the ratio of the 1064-nm to 532-nm attenuated backscatter). Dust aerosols have large VDR values and color ratios due to nonsphericity and to relatively large particle sizes, respectively. Other types of aerosols typically have small VDR values [*D. Liu et al.,* 2008; *Z. Liu et al.,* 2008]. For pollution aerosols, extinction at 532 nm is larger than that at 1064 nm. The values of the three parameters plotted in Figures 2b-d indicate the presence of dust aerosols, and the cloud mask in Figure 2a denotes the presence of cloud. The CALIPSO data indicate that the aerosols are mostly dust. Using the information from all four panels in Figure 2, we can define the cloud as a dusty cloud, which is denoted by the black rectangle.

A similar observation, shown in Figure 3, from April 18, 2007 shows a dusty cloud in the remote region. The CALIPSO data (Figures 3b-d) show that the feature identified as a low-confidence cloud

by CloudSat (Figure 3a) has dust aerosols in the same layers next to and below it. Figures 2 and 3, illustrate that dusty clouds exist in both the source and remote regions. Table 1 lists the 20 dusty cloud cases for each region that were selected for this study.

4. Comparative Analysis

To explore their differences, the physical properties of dusty clouds were compared with those of pure clouds in the source and remote regions. Histograms of the liquid water and ice cloud properties for each category from the 40 cases in Table 1 are shown in Figures 4 through 9 to illustrate any differences. These figures help determine the possible influences of dust aerosols on water and ice cloud properties, such as optical depth, effective particle size, LWP, and IWP. Figure 4 shows the frequency distributions of dusty and pure cloud optical depths in the source and remote regions. For water clouds in the source and remote regions, the respective mean optical depths for pure clouds are 6.8 and 15.0, values that are 16.6% and 21.1% larger than for dusty clouds. For ice clouds the mean optical depth for pure clouds is 8.9, which is negligibly greater than that for dusty clouds in the source region. In the remote region, the mean optical depth for pure clouds is 15.8, which is 29.5% larger than the dusty cloud optical depth. In addition, smaller values of optical depth occur more frequently for dusty clouds in both the source and remote regions.

The frequency distributions of water droplet radius and ice particle diameter for pure and dusty clouds are shown in Figure 5. The mean droplet radius for pure clouds in the source region (Figure 5a) is 11.7 μm compared to 9.3 μm for dusty clouds. In the remote region (Figure 5b), however, the mean droplet radii for pure clouds are much the same, differing by only 1.6%. The mean *Re* for pure clouds is approximately the same for both source and remote areas, but the average droplet radius for dusty

clouds in the source region is less than in the remote region. As shown in Figure 5c, the mean particle diameter for pure clouds is 44.0 μm in the source region, while the dusty cloud mean is 35.7 μm, a decrease of 18.9%. In the remote region (Figure 5d), the mean *De* for pure clouds is 55.3 μm compared to 51.7 μm for dusty clouds, a decrease of 6.5%.

These results clearly show that, in comparison to pure clouds, smaller values of mean *Re* occur more frequently for dusty clouds in both the source and remote regions. This difference is likely due to the dust aerosols reducing the size of the cloud particles by increasing the number of available CCN. The negligible difference in *Re* over the remote region is surprising. However, a number of factors may cause the similarities between the dusty and pure clouds. At low levels, the dust loading in the remote region is 4-5 times smaller than over the source regions [*Huang et al*., 2008], probably due to fallout or washout of the dust at low levels by the time the air reaches the coast. The finer dust aloft is carried much farther and higher by strong winds, and, therefore, would affect the high clouds but not the low clouds. Furthermore, the remote region is heavily polluted with a variety of aerosols from anthropogenic sources. The presence of those aerosols would diminish the susceptibility of the clouds to further changes in the cloud microphysical properties. Thus, the dust would have negligible impact on the low clouds in the remote region.

LWP and IWP are computed from the cloud optical depths and effective particle sizes. The resulting mean values of LWP and IWP for dusty clouds are considerably smaller than those for pure clouds (Figure 6). The averaged LWP decreases from 48.3 g/m^2 for pure clouds to 33.3 g/m^2 for dusty clouds (-31.2%) in the source region (Figure 6a), and decreases from 101.7 g/m^2 to 74.1 g/m^2 in remote region for pure and dusty clouds, respectively (Figure 6b). Similar drops are seen in the IWP means. In the source region (Figure 6c), the mean IWP decreases from 139.1 g/m^2 (pure clouds) to

108.6 g/m^2 (dusty clouds), while it decreases considerably, from 273.2 g/m^2 to 185.0 g/m^2, in the remote region (Figure 6d). Smaller values of LWP and IWP occur more frequently in dusty clouds than in pure clouds.

With the exception of the low-level clouds in the remote region, the results shown in Figures 4 through 6 show that the mean values of dusty cloud IWP, droplet radius and particle diameter are all less than those observed for pure clouds in both the source and remote regions. This strongly suggests that dust aerosols impact the cloud microphysical properties. However, the cloud properties are also affected by a variety of other factors, especially the thickness of moist layer giving rise to the observed cloud. To examine the humidity impact, the mean relative humidity was computed from the NCEP analyses for the 50-hPa layers above and below the cloud-top. Overall, as seen in Table 2, the mean column relative humidities are essentially the same for both pure and dusty clouds, but the remote region is 50% more humid than the source region. In the source region, the relative humidity ±50 hPa within the dusty cloud tops is 49%, which is 15% less than for the pure clouds. The relative humidity 50 hPa above dusty clouds is 17.7% less than for pure cloud, but below the dusty clouds the relative humidity is only 1.4% less than for pure clouds (as show in table 3). These results suggest that, in the source regions, the supersaturated layers are thicker for the pure clouds than for the dusty clouds. A thicker supersaturated layer implies a greater optical depth than for the pure cloud.

This humidity difference could explain the slightly larger optical depths of the liquid water clouds and could affect the particle size because thicker clouds allow for more growth of a droplet as an air parcel rises through the cloud. However, since the mean ice cloud optical depths in the source region are nearly identical, the humidity field differences are unimportant. Thus, it is concluded that the difference in Re and LWP are primarily due to the dust aerosol increasing the concentrations of

condensation nuclei in the dusty clouds. The small differences in mean relative humidity for the dusty and pure clouds in the remote region probably cannot account for the ~35% difference between the pure and dusty cloud optical depths. For ice clouds, it is also concluded that the difference in De and IWP are primarily due to the dust aerosol increasing the concentrations of ice nuclei in the dusty clouds.

This idea is confirmed in Figure 7, which shows a comparison of Re and De as functions of LWP and IWP (c, d) between dusty and pure clouds over the source and remote regions. In the source region, Re (De) for dusty clouds is less than for pure cloud for the same LWP (IWP) bin, it means that when dust particles are entrained in the clouds, the increased dust aerosol concentrations greatly increases the quantity of cloud CCN, this effect distributes water vapor between more dust particles. Thus, the effective radius of cloud droplets will consequentially be sharply reduced (*Rosenfeld et al*., 2001; *Twomey*, 1974). In the remote region, the results are the same, but the dust effects are less noticeable than in the source region. In addition, in source region, the Re (De) for dust polluted cloud is smaller than for pure clouds having the same optical depths (see Figure 8). These results confirm that when dust particles are involved in cloud development as CCN and IN at the same time, they diminish the cloud particle sizes, but have less effect in the remote region than in the source region presumably because the clouds in the former region are less susceptible to the inclusion of additional CCN or IN.

The frequency distributions of mean effective temperature for dusty and pure clouds in the source and remote regions are shown in Figure 9. The temperatures for dusty clouds in both regions are similar but slightly higher than those for pure clouds, indicating that the top heights of the dusty clouds are lower than for pure clouds. Under partly cloudy conditions, the satellite-retrieved cloud properties may be underestimated or overestimated due to the presence of dust aerosols and partially cloud-filled

pixels, resulting in higher reflectance and warmer brightness temperatures. Comparison of the results in the source and remote regions indicates that dust aerosols have less impact on clouds in the remote region than in the source region, as expected. This indicates that the character and impact of the dust aerosols change as they advect into the remote region.

The cloud radiative forcing is defined as the difference between the clear-sky and the total-scene radiation results [*Ramanathan et al.*, 1989].

$$C_{sw} = F_{clr}^{sw} - F_{sw},$$

$$C_{lw} = F_{clr}^{lw} - F_{lw},$$

and

$$C_{net} = C_{sw} + C_{lw},$$

where F_{clr}^{sw} and F_{clr}^{lw} are the CERES clear sky broadband SW and LW radiative fluxes at the TOA, respectively, F_{sw} and F_{lw} are SW and LW RF at the TOA for clouds (including dusty clouds) and for no cloud observation. The NET RF of TOA for pure and dusty clouds in the source and remote regions is shown in Figure 10. For water clouds, the NET RF for dusty clouds (D_W) is -52.4 W/m^2, which is about 36.9% greater than for pure clouds (P_W) in the source region. In the remote region, the NET RF for dusty clouds (D_W) is -208.0 W/m^2, which is about 14.3% greater than for pure clouds (P_W). For ice clouds, the NET RF for dusty clouds (D_I) is -56.9 W/m^2 in the source region, which is about 46.0% greater than for pure clouds (P_ I). In the remote region, the NET RF for dusty clouds (D_ I) is -230.6 W/m^2, which is about 15.9% greater than for pure clouds (P_ I). These results demonstrate that the NET cloud RF is reduced by dust aerosols at the TOA, and that the dust aerosols also inhibit the cooling effect of clouds. This effect is greater in the source region than in the remote area. In addition, the absolute values of NET RF for dusty and pure clouds (both water and ice clouds)

in the remote region are both larger than in the source region. This is due to the fact that RF at the TOA is not only affected by the spatial distribution of clouds, but also depends on other factors, including surface albedo, the optical properties of the aerosols and clouds, and the available moisture. The surface albedo is less in the Pacific Region (6-8%) than in the continental region (25%-35%), this is also one of the reasons that the largest negative RF values often appear over the ocean. The smaller optical depths of the dusty clouds would cause slightly less SW forcing than those of the pure clouds.

The instantaneous SW RF, LW RF and NET RF are shown as functions of effective temperature in the source and remote regions for water and ice clouds in Figures 11 and 12, respectively. For both water and ice clouds, the absolute values of RF (SW, NET and LW) decreased with increasing effective temperature, and the absolute values of RF (SW, LW and NET) for dusty clouds are less than those of pure clouds in both the source and remote regions. This behavior is not surprising due to the effect of dust aerosols on cloud and radiative properties. In addition, the difference of humidity in source and remote region is also one of the reasons (as show in table 2 and 3).

5. Discussion and Conclusions

Mineral dust aerosols are an important component of the Earth's climate system, possibly acting to accelerate the aridification of northern China. Dust generated in the Taklimakan and Gobi Deserts, and Asian pollution can become entrained and transported by westerly jets across eastern Asia, the Pacific Ocean, and may even reach North America. Dust plumes often pass through Pacific Ocean extra-tropical cloud systems, which are important climate regulators due to their large radiative cooling effect. The effect of this mixed dust-pollution plume on Pacific cloud systems and their associated RF is an unexplored, yet key factor for understanding climate change. In this study, the case studies and

statistical analyses document different dust effects on clouds over the source and remote regions during the PACDEX period (March through May, 2007), a season that is typically active for dust event development. The geographical locations of these study areas represent the upstream portion of the PACDEX regions of interest.

In this study, the results show that the impact of dust aerosols on cloud properties and RF is very complex. Dust aerosols appear to change the microphysical characteristics of clouds, reducing cloud optical depth, LWP, IWP and effective particle size. This implies that dust aerosols might be an important factor for suppressing precipitation by reducing the opportunity for the development of the larger hydrometeors necessary for precipitation. Once these aerosols enter the cloud in a dust storm or dust devil, they will participate in the cloud physical processes as CCN, thus greatly increases the CCN concentrations, reducing the effective radius of cloud droplets, and suppressing the occurrence of precipitation. However, the decreased cloud optical depth and water path reduce the cloud cooling effect, in essence causing an increased warming effect. These impacts are greater in the source region than in the remote region. The instantaneous net cloud cooling effect is reduced by 43.4% and 16.7% in the source and remote regions, respectively. Another possible mechanism of dust impact on climate is through the semi-direct effect, which is related to the absorption of solar radiation by dust aerosols [*Huang et al*., 2006b]. The absorption or diabatic heating of Asian dusts can cause the evaporation of cloud droplets and reduce cloud water path. Due to the large spatial and temporal extent of desert dust in the atmosphere, the interactions of desert dust with clouds can have substantial climatic impacts. The decreasing cloud optical depth and water path partially reduces the cloud cooling thus increasing the warming. It has been commonly believed that the desert dust might contribute significantly to the observed reductions in cloud droplet size and precipitation over Africa [*Rosenfeld et al*., 2001].

However, semi-direct effect may be dominated dust aerosol-cloud interaction over arid and semi-arid areas in East Asia, and contribute to reduce precipitation via a significantly different mechanism compared to that in Africa. Dust aerosols may have contributed to the desertification of northwestern China during recent decades [*Huang et al,* 2006b].

This study also demonstrated that dust aerosol effects on ice cloud are greater than on water clouds in the remote region. For example, in the remote region mean dusty water cloud droplet radius was 11.7 μm, which is only 2% less than for pure clouds in this region. However, the ice cloud particle diameter for pure clouds was 55.3 μm compared to 51.7 μm for dusty clouds, a decrease of 6.5%. These results are consistent with PACDEX aircraft observations. *Stith et al*. [2009] found that dust plumes had only a small impact on total cloud condensation nuclei (CCN), at sampling super saturations, but did exhibit high concentrations of Ice Nuclei (IN). IN concentrations in dust plumes exceeded typical tropospheric values by 4 to 20 times and were similar to previous studies of the Saharan Aerosol Layer (SAL). Enhanced IN concentrations were found in the upper troposphere off the coast of North America, providing a first direct validation of the transport of dust layers containing high IN near the tropopause entering the North American continent from distant sources [*Stith et al.*, 2009].

Although this study indicates that the dust effects on cloud and raditive properties are less in remote region than that in source region, the impact of long range transport of dust and air pollution from their continental sources over the oceanic regions is, however, one of the outstanding problems in regional and global climate change. Dust mixed with air pollution leads to a brownish haze, which absorbs and scatters sunlight and leads to a large reduction of sunlight at the surface [*Ramanathan*, et al., 2001] resulting in so-called “global dimming.” The vertical structure and degree of vertical mixing between dust and pollution layers as they are transported is, however, poorly known. The widespread dust and

pollution over the northern Pacific Ocean makes it one of the largest pollution-affected oceanic regions of the world, at least, during spring time. This transport is quite efficient, sometimes transporting the hazy mixture across the Pacific from Asia to North America. Because of the fast large-scale transport in the upper troposphere, once aerosols, such as dust and black carbon enter the upper troposphere (above 8 km), they can be transported around the earth in a latitudinal belt within 1 to 2 weeks. As a result, dust from Asia can impact upper tropospheric clouds over North America and the Atlantic as well. For example, *Demott et al*. [2003] use CRYSTAL-FACE data to suggest that fine dust from North Africa contributed significantly to ice nuclei populations over Florida. Using ground-based lidar polarization data, *Sassen*, *et al*. [2002] found that Asian dust affected the formation and phase of ice clouds, leading to unusually warm cirrus clouds. Several studies have reported that dust aerosols generated in the Taklimakan and Gobi areas can be transported eastward by prevailing westerlies over China, North and South Korea, and Japan, [*Iwasaka et al*., 1983; *Zhang et al*., 1997; *Murayama et al*., 2001; *Uno et al*., 2001; *Natsagdorj et al*., 2003, *Huang et al*., 2008], and are carried even farther across the Pacific Ocean reaching the North America [*Uno et al*., 2001; *Husar et al*., 2001; *Sassen*, 2002], Asia dust effects on the remote region 's cloud and radiative properties still need to be further explored for more detail.

The conclusions from this study are only based on satellite and in-situ measurements taken during the PACDEX (March – May 2007) field experiment and do not cover a sufficient time span to definitively quantify the observed dust effect on clouds over such two regions. Long term monitoring and analysis is necessary to determine the full scope of these effects. Since dust direct radiative effects are important in modulating global and regional climate. Further research should focus on combining A-Train satellite measurements with PACDEX aircraft and surface sites measurements.

1

Acknowledgments: This research was supported by the National Science Foundation of China under grants 40725015 and 40633017 and by the NASA Science Mission through the CALIPSO Project and the Radiation Sciences Program. The CALIPSO, CERES SSF, and CloudSat data were obtained from the NASA Earth Observing System Data and Information System, Atmospheric Sciences Data Center (ASDC) at Langley Research Center.

References

Chen, L., Yin, Y., Yang, J, Niu, S.J (2007). Effects of sand dust particles on cloud and precipitation: a numerical study. *Journal of Nanjing Institute of Meteorology 30*(5), 590-600.

Collins, W.D., W. C. Conant, and V. Ramanathan (1994), Earth radiation budget, clouds and climate sensitivity.In: *The Chemistry of the Atmosphere: Its Impact on Global Change* (ed. Calvert J. G.). Oxford: Blackwell Scientific Publishers, 207-215.

DeMott, P. J., K. Sassen, M. R. Poellot, D. Baumgardner, D. C. Rogers, S. D. Brooks, A. J. Prenni, and S. M. Kreidenweis (2003), African dust aerosols as atmospheric ice nuclei, *Geophys. Res. Lett.*, *30*(14), 1732, doi:10.1029/2003GL017410.

Han, Y. X., Chen Y. H., Fang, X. M., Zhao, T. L., (2008), The possible effect of aerosol on precipitation in Trim basin, *China Environmental Science*, *28* (2), 102-106.

Hu, Y., Z. Liu, D. Winker, M. Vaughan, V. Noel, L. Bissonnette, G. Roy and M. McGill, (2006), A simple relation between lidar multiple scattering and depolarization for water clouds, *Optics Letters*, *31*, 1809-1811.

Huang, J., P. Minnis, B. Lin, T. Wang, Y. Yi, Y. Hu, S. Sun-Mack, and K. Ayers (2006a), Possible influences of Asian dust aerosols on cloud properties and radiative forcing observed from MODIS and CERES, *Geophys. Res. Lett.*, *33*, L06824, doi: 10.1029/2005GL024724.

Huang, J., B. Lin, P. Minnis, T. Wang, X. Wang, Y. Hu, Y. Yi, and J. K. Ayers (2006b), Satellite-based assessment of possible dust aerosols semidirect effect on cloud water path over East Asia, Geophys. Res. Lett., 33,L19802, doi:10.1029/2006GL026561.

Huang, J., et al. (2007), Summer dust aerosols detected from the CALIPSO satellite over the Tibetan Plateau, *Geophys. Res. Lett.*, *34*, L18805, doi: 10.1029/2007GL029938R.

Huang, J., P. Minnis, B. Chen, Z. Huang, Z. Liu, Q. Zhao, Y. Yi, and J. K. Ayers (2008), Long-range transport and vertical structure of Asian dust from CALIPSO and surface measurements during PACDEX, *J. Geophys. Res.*, 113, D23212, doi:10.1029/2008JD010620.

Husar R. B., et al. (2001), Asian dust events of April 1998, *J. Geophys. Res.*, *106*, 18317-18330.

Iwasaka, Y., H. Minoura, and K. Nagaya (1983), The transport and spatial scale of Asian dust-storm clouds: A case study of the dust-storm event of April 1979, *Tellus*, *Ser. B*, *35*, 189–196.

Kalnay, E., et al. (1996), The NCEP/NCAR 40-year reanalysis project, *Bull. Am. Meteorol. Soc.*,*77*, 437-471.

Li, Z (2004), Aerosol and climate: A perspective from East Asia. In: *Observation, Theory, and Modeling of the Atmospheric Variability* (ed. Zhu D.). Singapore: World Scientific Pub. Co., 501-525

Liu, D., Z. Wang, Z. Liu, D. Winker, and C. Trepte (2008), A height resolved global view of dust aerosols from the first year CALIPSO lidar measurements, submitted to *J. Geophys. Res*.

Liu, Z., W. Hunt. M. Vaughan, C. Hostetler, M. McGill, K. Powell, D. Winker, and Y. Hu. (2006), Estimating random errors due to shot noise in backscatter lidar observations, *Appl. Opt.*, *45*, 4437-4447.

Liu, Z., A. Omar, M. Vaughan, et al. (2008), CALIPSO lidar observations of optical properties of Saharan dust: A case study of long range transport, *J. Geophys. Res.*, in press.

Loeb, N.G., S. Kato, K. Loukachine, and N. Manalo-Smith (2005), Angular distribution models for top-of-atmosphere radiative flux estimation from the Clouds and Earth's Radiant Energy System instrument on the Terra satellite. Part 1: Methodology, *J. Atmos. Ocean Tech.*, *22*, 338-351.

Mace, G. G., R. Marchand, Q. Zhang, and G. Stephens (2007), Global hydrometeor occurrence as observed by Cloudsat: Initial observations from Summer 2006, *Geophys. Res. Lett.*, *34*, 10 L09808, doi:10.1029/2006GL029017.

Minnis, P., et al. (2008), Cloud detection in non-polar regions for CERES using TRMM VIRS and Terra and Aqua MODIS data, *IEEE Trans. Geosci. Remote Sens.*, *46*, 3857-3884.

Minnis, P., et al. (2009), Cloud property retrievals for CERES using TRMM VIRS and Terra and Aqua MODIS data, *IEEE Trans. Geosci. Remote Sens.*, submitted.

Murayama, T., et al.(2001), Ground-based network observation of Asian dust events of April 1998 in east Asia, *J. Geophys. Res.*, *106* (D16), 18345–18360.

Natsagdorj, L., D. Jugder, Y.S. Chung (2003), Analysis of dust storms observed in Mongolia during 1937–1999, *Atmos. Environ. 37*, 1401–1411.

Niu S. J. (2001), Researches on the distribution of dust aerosols particle spectrum in Helan Mountain area, *Atmos. Sci.*, *25*, 242-252

Ramanathan V., Cess R. D., Harrison E. F., et al. (1989), Cloud radiative forcing and climate: results from the Earth Radiation Budget Experiment, *Science*, *243*, 57-63.

Ramanathan, V., et al. (2001), Indian Ocean experiment: An integrated analysis of the climate forcing and effects of the great Indo-Asian haze, *J. Geophys. Res.*, *106*(D22), 28,371 – 28,398.

Ramaswamy V., Boucher O., Haigh J., et al. (2001), Radiative forcing of climate change, in climate change (2001). The Scientific Basis, Contribution of Working Group I to Third Assessment Report of the Intergovernmental Panel on Climate Change (eds. Houghton J. T., Ding Y., Griggs D. J. et al.), *New York, Cambridge Univ. Press*, 349-416.

Rosenfeld, D., Rudich, Y., Lahav, R., (2001), Desert dust suppressing precipitation-a possible desertification feedback loop, *Proceedings of the National Academy of Sciences, 98*, 5975-5980.

Sassen, K. (2002), Indirect climate forcing over the western US from Asian dust storms. *Geophys. Res. Lett.*, *29*, 10.1029.

Stephens, G. L., et al. (2002), The Cloudsat Mission and the A-Train: A new dimension of space-based observations of clouds and precipitation, *Bull. Amer. Meteor. Soc.*, *83*, 1771-1790.

Stith, J. L., V. Ramanathan, W. A. Cooper, G. Roberts, P. J. DeMott, G. Carmichael, (2009), An Overview of Aircraft Observations from the PACDEX Campaign, *To be published in JGR.*

Twomey, S., (1974): Pollution and the planetary albedo. *Atmospheric Research*, *8*, 1251-1256.

Uno, I., H. Amano, S. Emori, K. Kinoshita, I. Matsui, N. Sugimoto (2001), Trans- Pacific yellow sand transport observed in April 1998: A numerical simulation, *J. Geophys. Res.*, *106*(D16), 18331-18344,10.1029/2000JD900748.

Vaughan, M., et al. (2004), Fully automated analysis of space-based lidar data: An overview of the CALIPSO retrieval algorithms and data products, *Proc. SPIE Int. Soc. Opt. Eng.*, *5575*, 16-30.

Wielicki, B. A., et al. (1998), Clouds and the Earth's Radiant Energy System (CERES): Algorithm overview, *IEEE Trans. Geosci. Remote Sens.*, *36*, 1127-1141.

William, J. R,. F. Wu, D. J. Gaffen (2000), Interannual variability of the tropical tropopause derived from radiosonde data and NCEP reananlyses, *J. Geophys. Res.*, *105* (D12), 15509–15523.

Winker, D. M., W. H. Hunt, and M. J. McGill (2007), Initial performance assessment of CALIOP, *Geophys. Res. Lett.*, *34*, L19803, doi: 10.1029/2007GL030135.

Yin, Y., Chen, L., (2007), The effects of heating by transported dust layers on cloud and precipitation : a numerical study. *Atmospheric Chemistryand Physics.*, *7*, 3497-3505

Zhang, X. Y., R. Arimoto, and Z. S. An (1997), Dust emission from Chinese desert sources linked to variations in atmospheric circulation, *J. Geophys. Res.*, *102*(D23), 28,041–28,044.

Zhang, X. Y., et al. (2003), Characterization of soil dust aerosol in China and its transport and distribution during 2001 ACE Asia: Network observations. *J. Geophys. Res.*, *108* (D9), 4261, doi: 10.1029/2002JD002632.

Zhou, Z. Q.(2001), Sand and dusty storm weather of China in recently 45 years, *Quaternary Res.*, *21* (1), 9-16.

Figure Captions

Figure 1.Regions selected to compare dust aerosol effect on cloud properties and cloud radiative forcing.

Figure 2.Vertical profiles of dusty cloud parameters in the source region, March 5, 2007. (a) Cloudsat cloud mask image, (b) CALIPSO 532-nm total backscatter, (c) volume depolarization ratio, and (d) 1064-nm/532-nm backscatter color ratio.

Figure 3.Same as Figure 2, but for April 18, 2007 in the remote region.

Figure 4.Comparison of water (a, b) and ice cloud (c, d) optical depths between the source (a, c) and remote (b, d) regions.

Figure 5.Same as Figure 4 but for water droplet radius and ice particle diameter. The histogram intervals are 4 μm for droplet radius and 20 μm for particle diameter.

Figure 6.Same as Figure 4 but for liquid water path (LWP) and ice water path (IWP). The histogram intervals are 100 g/m^2 for LWP and 300 g/m^2 for IWP.

Figure 7.Comparison of Re(a, b) and De (c, d) as a function of LWP and IWP between dusty and pure cloud over the source (a, c) and remote (b, d) regions.

Figure 8.Comparison of Re(a, b) and De (c, d) as a function of water and ice cloud optical depths between dusty and pure cloud over the source (a, c) and remote (b, d) regions.

Figure 9.Same as Figure 4 but for cloud effective temperature. The histogram intervals are 10 K for both water and ice clouds.

Figure 10.TOA NET radiative forcing of dusty and pure clouds in the source and remote regions.

Figure 11.Comparison of TOA SW, LW and NET radiative forcing as a function of effective temperature for water clouds between the source(a, c, e) and remote regions (b, d, f).

Figure 12.Same as Figure 11, but for ice clouds.

Table 1. Selected source and remote region dust cloud cases in 2007.

	Source Region				Remote Region			
Case	**Month Day**	**UTC Time**	**Latitude (°)**	**Longitude (°)**	**Month Day**	**UTC Time**	**Latitude (°)**	**Longitude (°)**
1	3-5	7:44	38.08-39.19	83.13-83.47	3-21	4:26	35.67-36.60	133.36-133.64
2	3-19	6:17	35.04-37.36	105.33-106.01	3-22	5:10	37.47-40.98	121.20-122.30
3	3-21	7:45	39.20-41.51	82.41-83.14	3-23	4:14	36.34-39.50	135.58-136.54
4	3-21	7:46	42.98-44.35	81.44-81.92	4-1	4:08	37.04-39.58	137.10-137.87
5	4-2	8:09	37.50-40.17	76.66-77.48	4-1	4:09	41.32-42.16	136.27-136.54
6	4-4	7:58	41.52-44.23	78.40-79.31	4-2	4:51	36.51-38.83	126.52-127.21
7	4-10	7:20	38.34-41.76	88.51-89.59	4-7	5:09	35.23-37.33	122.34-122.95
8	4-12	7:8??	39.54-43.00	91.18-92.31	4-7	5:11	41.64-43.73	120.28-120.99
9	4-20	7:57	38.49-41.12	79.46-80.28	4-8	4:15	39.66-43.22	134.36-135.53
10	4-21	7:02	40.31-42.58	92.88-93.62	4-8	4:16	43.26-44.90	133.77-134.35
11	4-22	7:45	39.85-42.16	82.21-82.96	4-10	4:02	37.39-40.90	138.23-139.32
12	5-1	7:38	37.21-39.97	84.46-85.31	4-11	4:45	36.46-39.71	127.79-128.77
13	5-6	6:19	41.40-44.24	103.12-104.09	4-11	4:46	41.18-43.58	126.52-127.32
14	5-6	7:57	38.04-41.51	79.33-80.42	4-18	4:51	36.1-39.35	126.36-127.34
15	5-14	7:07	36.68-39.48	92.34-93.19	5-4	4:51	35.94-39.41	126. 35-127.39
16	5-17	7:38	37.40-39.49	84.63-85.27	5-5	3:56	38.40-40.98	139. 76-140.57
17	5-20	6:30	36.20-38.74	101.85-102.61	5-11	3:18	35.16-36.01	150.55-150.79
18	5-22	6:18	39.17-41.04	104.21-104.80	5-14	3:50	39.78-42.22	140.89-141.69
19	5-22	7:57	38.13-39.15	80.09-80.40	5-20	4:51	35.81-38.35	126. 69-127.44
20	5-26	7:33	40.60-43.95	84.69-85.81	5-30	3:50	40.54-41.92	140.99-141.44

Table 2. Mean relative humidity of dusty and pure cloud in the source and remote regions.

Source Region		Remote Region	
Dusty Cloud (%)	**Pure Cloud (%)**	**Dusty Cloud (%)**	**Pure Cloud (%)**
50.01	52.98	75.76	78.29

Table 3. Mean relative humidities 50 hPa above and below the cloud top.

Source region (%)				**Remote region (%)**			
Dusty cloud		**Pure cloud**		**Dusty cloud**		**Pure cloud**	
below	above	below	above	below	above	below	above
48.3	49.6	55.2	60.3	61.2	51.1	62.1	55.8

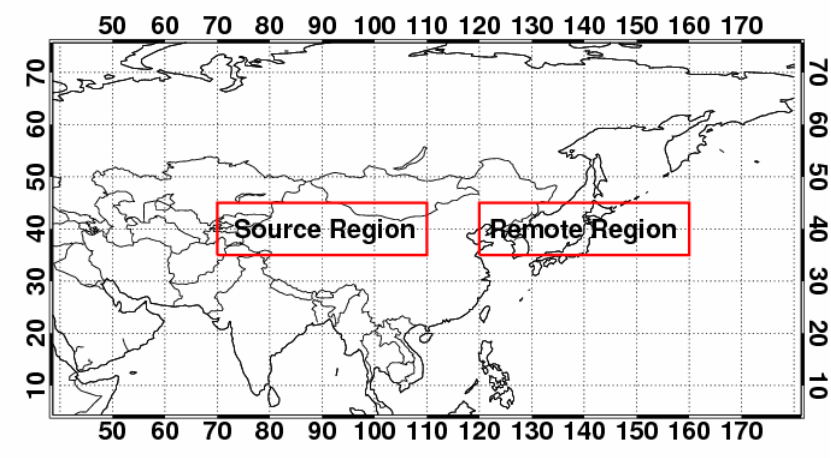

Figure 1. Regions selected to compare dust aerosol effect on cloud properties and cloud radiative forcing.

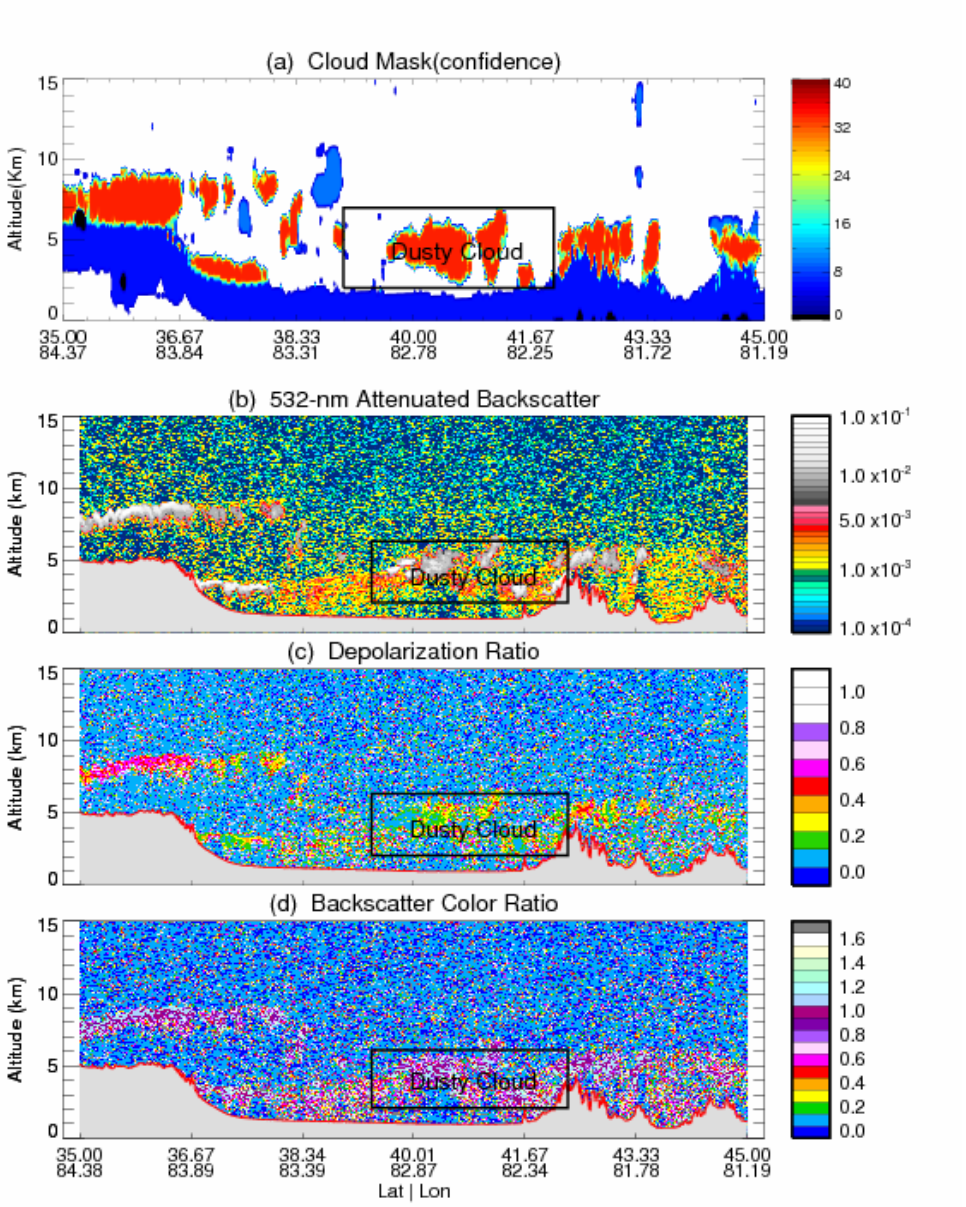

Figure 2. Vertical profiles of dusty cloud parameters in the source region, March 5, 2007. (a) Cloudsat cloud mask image, (b) CALIPSO 532-nm total backscatter, (c) volume depolarization ratio, and (d) 1064-nm/532-nm backscatter color ratio.

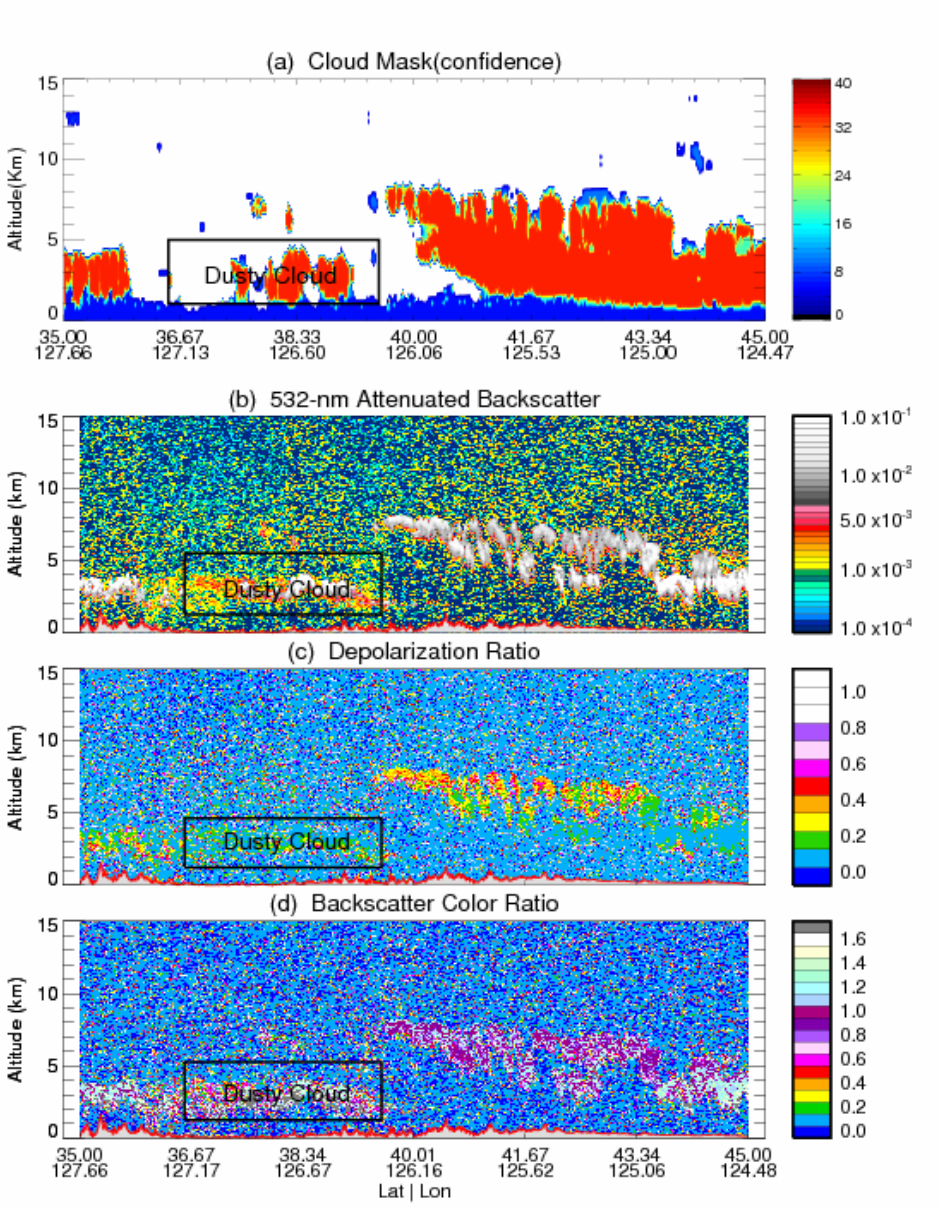

Figure 3. Same as Figure 2, but for April 18, 2007 in the remote region.

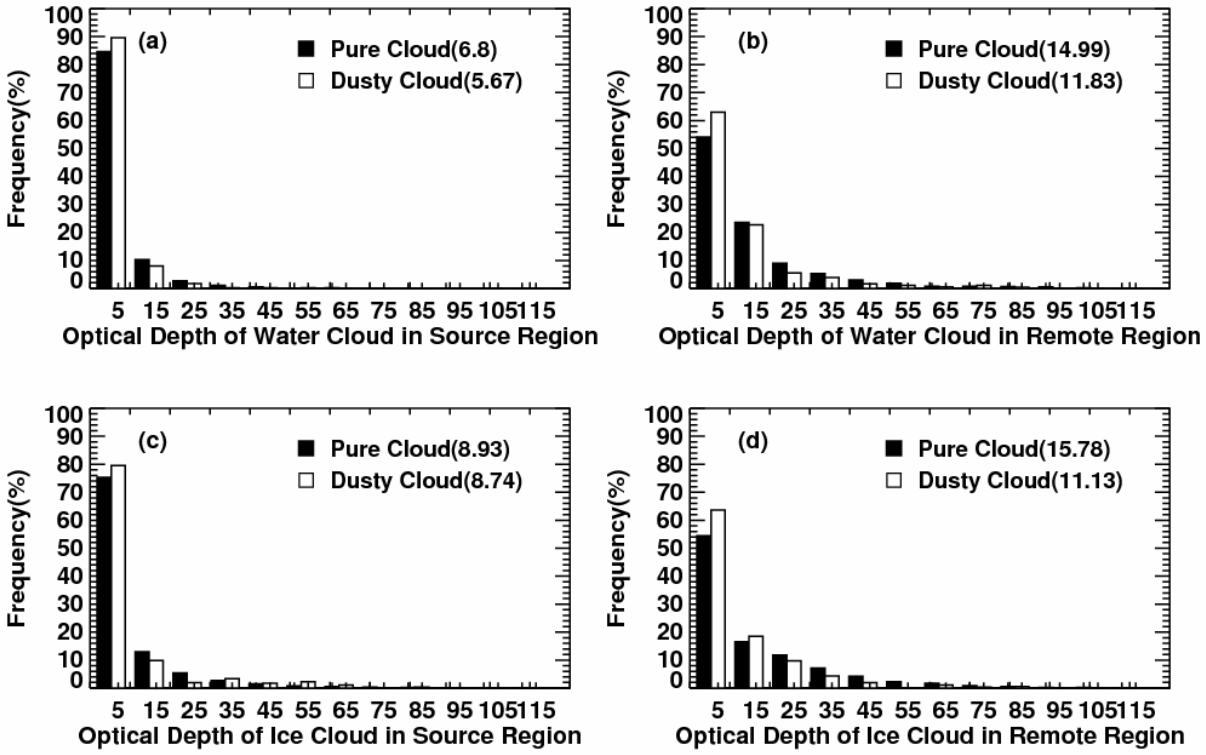

Figure 4. Comparison of water (a, b) and ice cloud (c, d) optical depths between the source (a, c) and remote (b, d) regions.

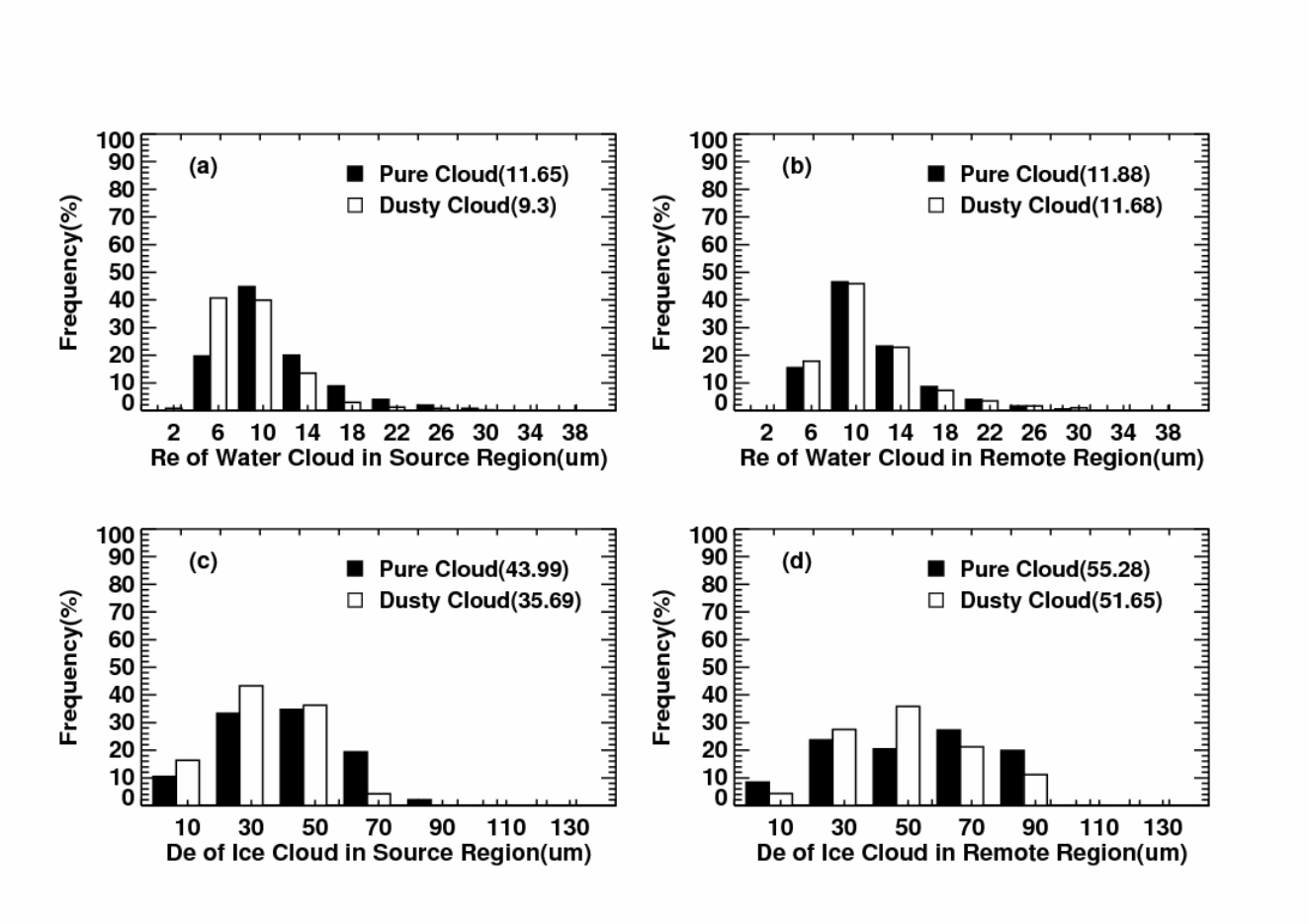

Figure 5. Same as Figure 4 but for water droplet radius and ice particle diameter .The histogram intervals are 4 μm for droplet radius and 20 μm for particle diameter.

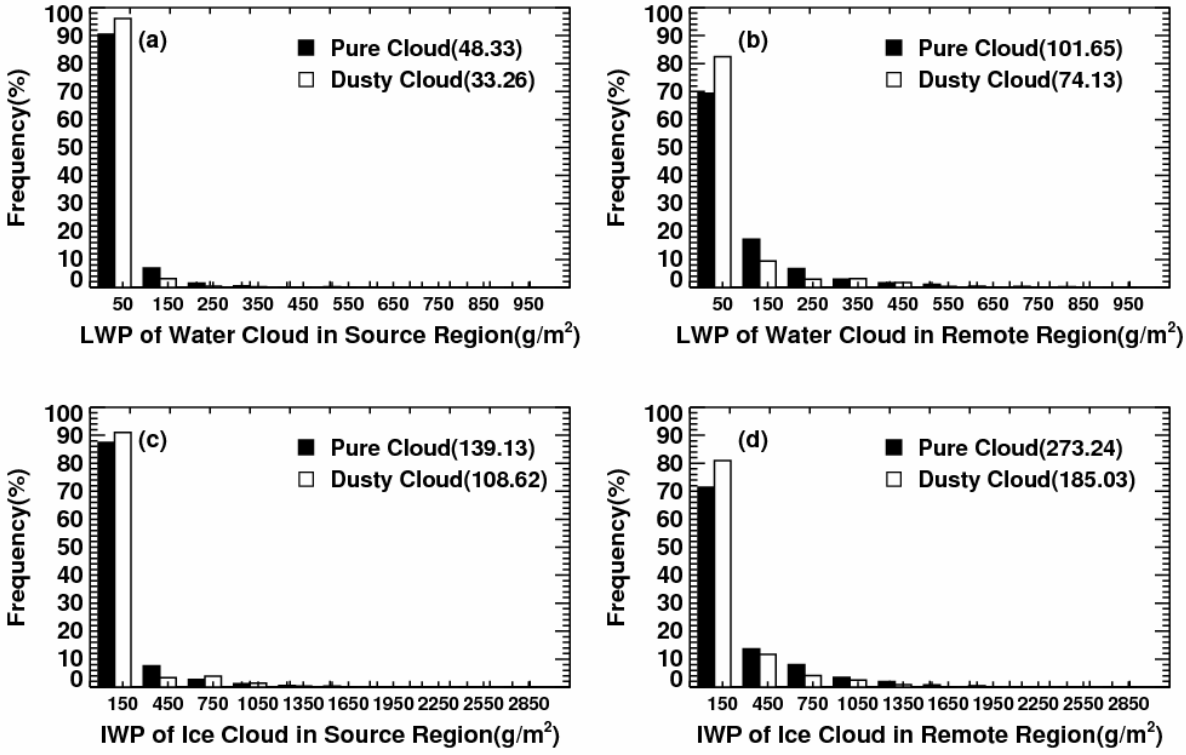

Figure 6. Same as Figure 4 but for liquid water path (LWP) and ice water path (IWP).The histogram intervals are 100 g/m^2 for LWP and 300 g/m^2 for IWP.

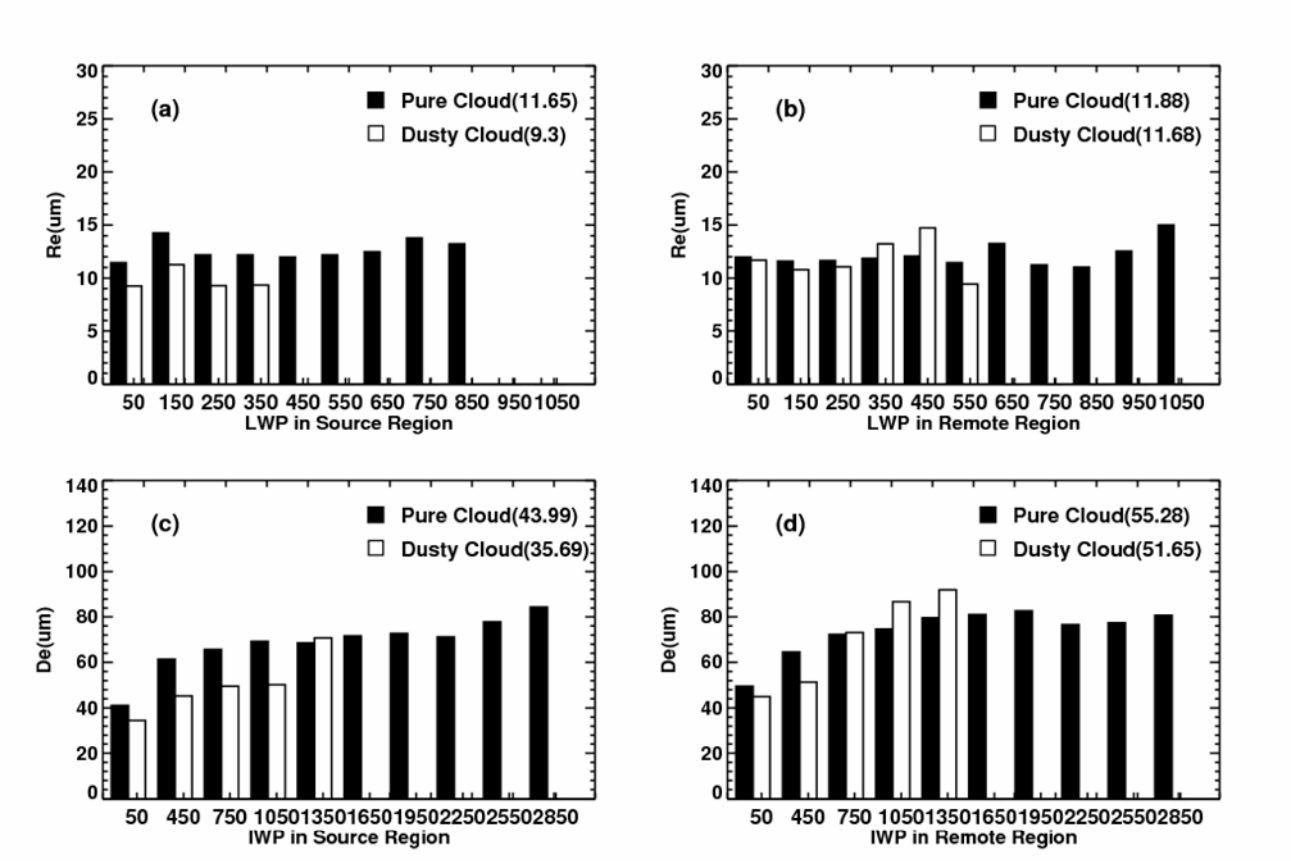

Figure 7. Comparison of Re(a, b) and De (c, d) as a function of LWP and IWP between dusty and pure cloud over the source (a, c) and remote (b, d) regions.

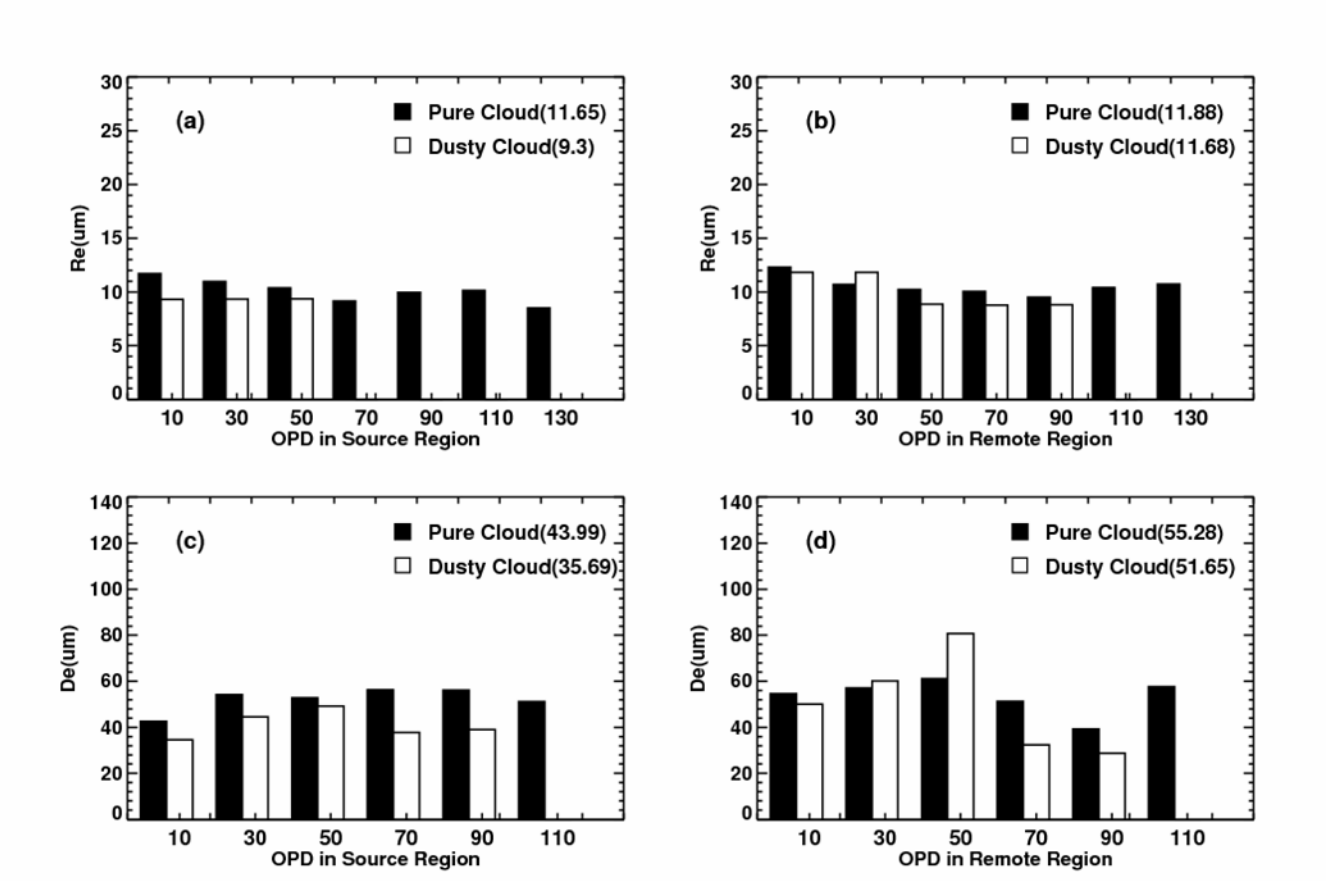

Figure 8. Comparison of Re (a, b) and De (c, d) as a function of water and ice cloud optical depths between dusty and pure cloud over the source (a, c) and remote (b, d) regions.

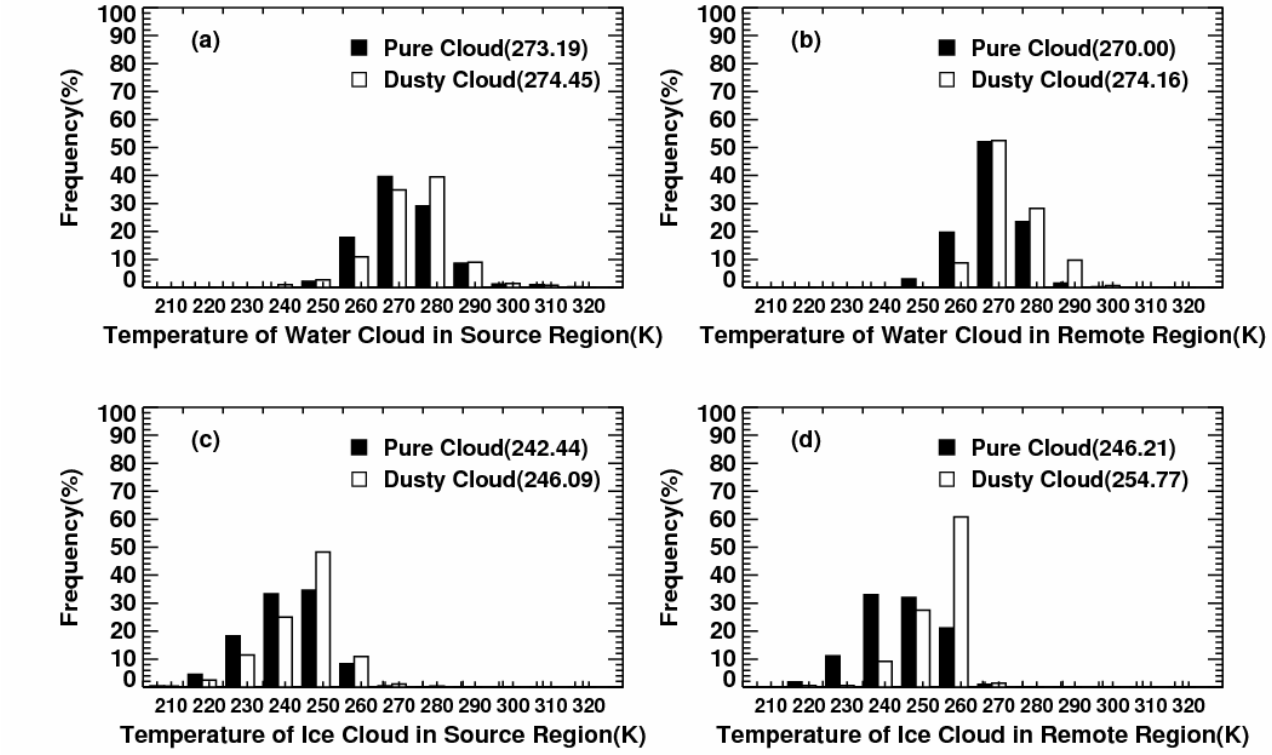

Figure 9. Same as Figure 4 but for cloud effective temperature.The histogram intervals are 10 K for both water and ice clouds.

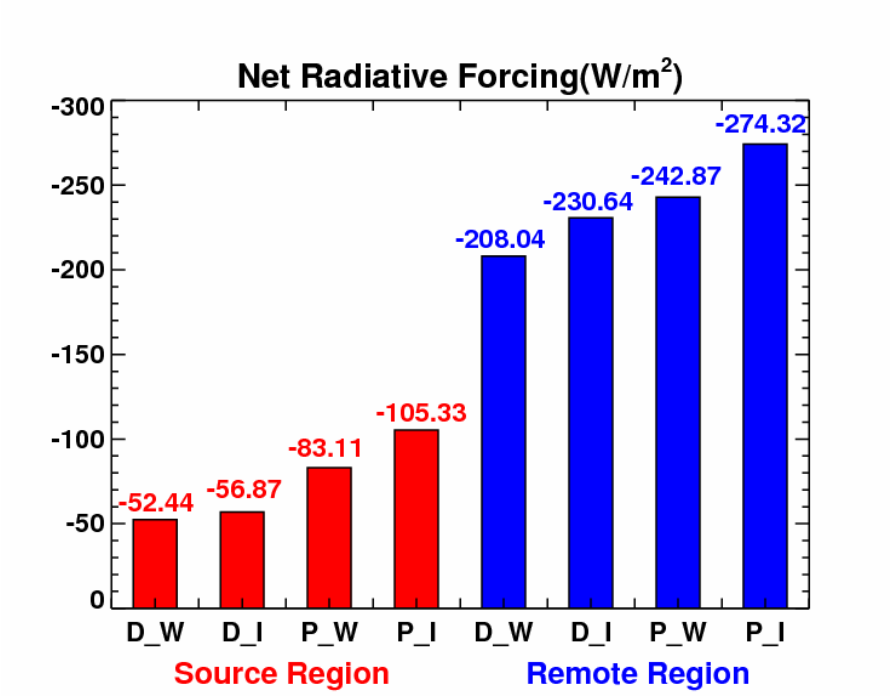

Figure 10. TOA NET radiative forcing of dusty and pure clouds in the source and remote regions.

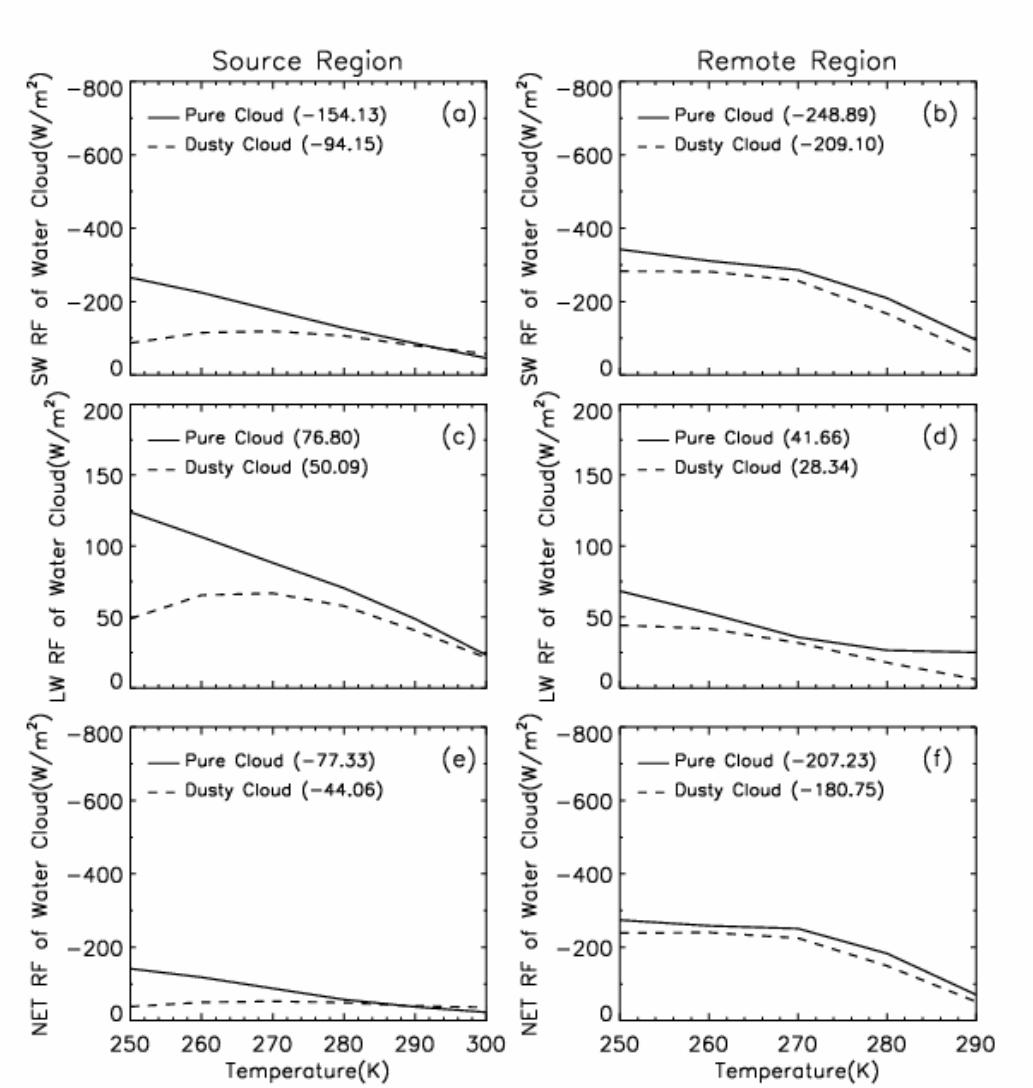

Figure 11. Comparison of TOA SW, LW and NET radiative forcing as a function of effective temperature for water clouds between the source (a, c, e) and remote regions (b, d, f).

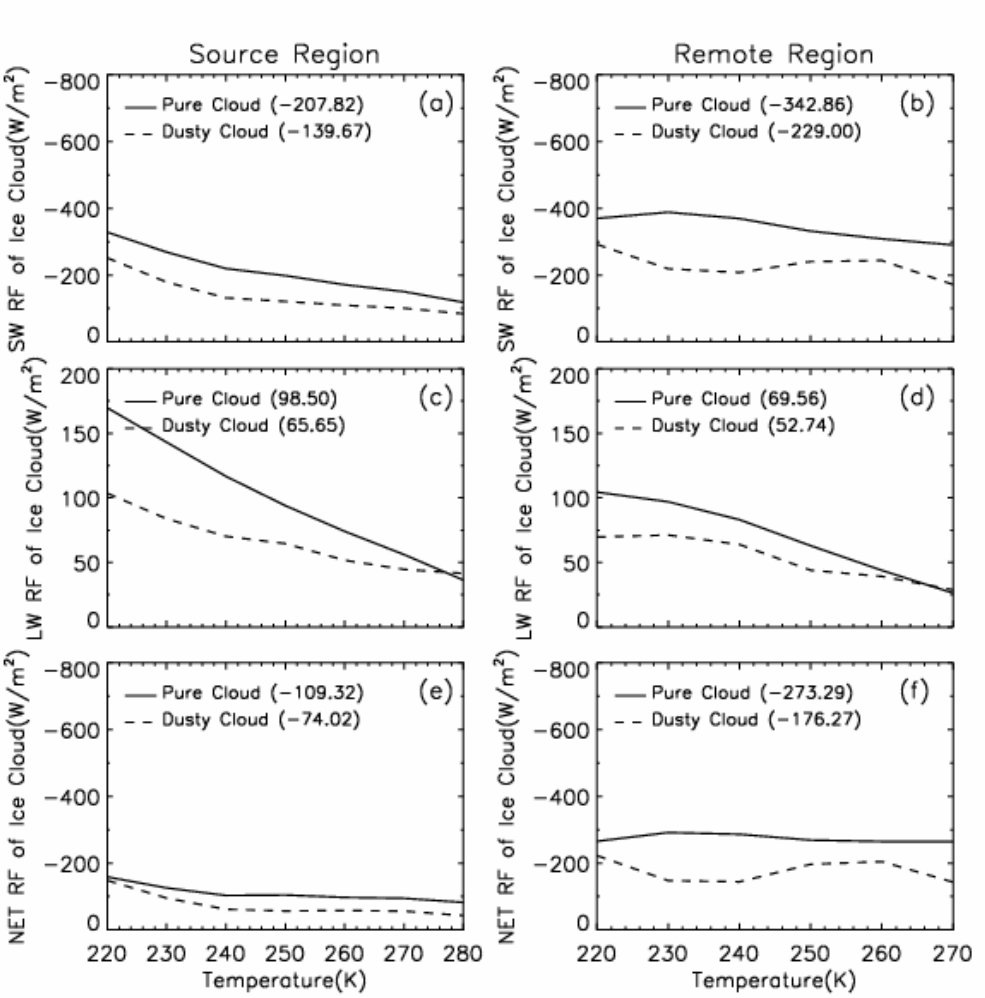

Figure 12. Same as Figure 11, but for ice clouds.